Bacterial exudate effects on Cu^{+2} sorption by cells: Quantifying significant ternary interactions.

Peter J. Swedlund[a], Magali Moreau[b] and Christopher J. Daughney[b]*

[a]School of Chemical Sciences, University of Auckland, Private Bag 92019, Auckland, New Zealand

[b]Institute of Geological and Nuclear Sciences, P.O. Box 30368, Lower Hutt, New Zealand

[*] Corresponding author p.swedlund@auckland.ac.nz

ABSTRACT

Bacteria exude a range of ligands which have diverse effects on trace metal geochemistry. This study evaluated the effect of ligands exuded by the bacterium *Anoxybacillus flavithermus* on the aqueous geochemistry of Cu^{+2}. Proton and Cu^{+2} binding by the exudate ligands were investigated via potentiometric titrations and polarographic studies respectively. Despite the apparent complexity of the system the Cu^{+2}-exudate interaction was well described by a single model reaction $H_2L + Cu^{+2} \Leftrightarrow LCu + 2H^+$. In a bacterial cell suspension the aqueous phase concentration of exudate ligands increased almost linearly with the age of the suspension. After 48 h the exuded ligands had roughly the same total binding capacity for Cu^{+2} as the cells from which they were derived. To investigate the significance of the exudate on Cu^{+2} uptake by the bacterial cells sorption experiments were conducted in ternary systems with bacterial cells and a range of concentrations of a well characterized exudate. The systems were modeled with the parameters derived from the binary Cu^{+2}-cells and Cu^{+2}-exudate experiments. Under conditions where the binary model parameters predicted that the exudate ligand would hold all of the Cu^{+2} in solution there was unexpectedly appreciable Cu^{+2} sorption by the cells. This indicated the presence of significant ternary interactions involving the Cu^{+2}, the cell surface sites and the exudate. The observations could be reasonably well described by adding to the binary model reactions a single reaction for a ternary complex with stoichiometry R_2CuLH^0 where R_2 represents a cell wall binding site. The exudate ligands produced by bacterial cells had a significant effect on Cu^{+2} partitioning between the solution and solid phases under the experimental conditions employed. However, the study shows that the strong complexes that exudate ligands can form with trace metals do not necessarily inhibit trace metal uptake by cells to the extent expected from first principles.

1. Introduction

Understanding trace metal chemistry in aquatic systems is both scientifically challenging and practically important. It is especially important to understand trace metal distribution between the solution and solid phases because this determines the ultimate fate of trace metals in natural systems and also the efficacy of treatment systems for contaminated water. Partitioning of trace metals between the solution and solid phases is affected by complexation with a plethora of different organic or inorganic ligands that exist in aquatic systems and is typically not fully described by simply combining the interactions gleaned from binary systems with one cation binding component. For this reason laboratory studies of incrementally increasingly complex systems are needed to close gaps that exist in the understanding of trace metal behavior in real systems.

The diversity of organic ligands in aquatic systems means they are difficult to fully characterize (Mason, 2013) and have a range of functional groups that can bind cations. For example cation binding by humic substances predominantly involves phenolic and aromatic carboxylate groups (Fujii et al., 2014; Tipping, 2002). Small molecules, such as phthalate, salicylate or picolinate, that have these functional groups are used as simple analogues of humic substances (Boily et al., 2005; Davis and Leckie, 1978; Le Person et al., 2014). In ternary cation-ligand-iron oxide systems these ligands have been shown to either promote or inhibit cation sorption depending on the conditions. The ligands can promote cation sorption by forming surface ternary complexes and can inhibit cation sorption by forming stable cation-ligand solution phase complexes (Ali and Dzombak, 1996; Boily et al., 2005; Davis and Leckie, 1978; Song et al., 2008).

The sorption of cations to bacterial cells is a well-known and fairly general phenomenon (Borrok et al., 2004; Daughney et al., 2010) though little is known about how organic ligands affect this. In two studies the sorption of Cd^{+2} to bacterial cells was found to be inhibited by the presence of either phthalate (Song et al., 2009) or EDTA (Fein and Delea, 1999). In these cases the extent of this inhibition was accurately predicted using the binary system binding constants indicating no significant ternary interactions. Bacteria also exude ligands which range from simple small organic acids to macromolecules with molecular weights greater than 12,000 Da. These exuded ligands

include a diverse set of functional groups including alpha-hydroxy carboxylic acids, catechols and hydroxamates (Albrecht-Gary and Crumbliss, 1998; Andrews et al., 2003; Lombardi et al., 2005) and have been described as exhibiting "remarkably similar proton binding capacities to humic substances" (Seders and Fein, 2011). Many aspects of trace metal chemistry can be moderated by bacterial exudates, such as activity, redox potential, coordination, sorption and mineral dissolution processes (Babechuk et al., 2009; Dogan et al., 2011; Jackson et al., 2005; Nogueira et al., 2012; Ohnuki et al., 2007).

Despite the significance of exudates on cation chemistry there is, to our knowledge, only one study looking at exudate effects on cation sorption by microorganisms and this study is very striking. Gorman-Lewis et al. (2013) studied complexation of the neptunium(V) cation (NpO_2^+) by *Bacillus subtilis* endospores and their exudates which were dominated by dipicolinic acid (pyridine-2,6-dicarboxylic acid). The exudate formed such strong solution complexes with NpO_2^+ that cation sorption by the endospores actually decreased with increasing pH. This is a dramatic deviation from typical cation sorption to vegetative cells which increases with increasing pH due to cation-proton exchange at the sorption site.

Given such a striking result from the only study investigating the effect of bacterial exudates on cation sorption, the system warrants further study and this is the motivation of our investigation. We have used Cu^{+2} and the Gram positive bacterium *Anoxybacillus flavithermus* because Cu^{+2} sorption onto this bacterium has been extensively studied in our group providing a sound base on which to incrementally increase the complexity (Burnett et al., 2006a; Burnett et al., 2006b; Burnett et al., 2007; Heinrich et al., 2007). *A. flavithermus* is a thermophilic facultative anaerobe which has been fully described in Saw et al. (2008). The Cu-exudate and Cu-cell binary systems are first characterized prior to experiments that explore the behavior of Cu^{+2} in ternary systems containing both exudate and the bacterial cells. Polarography and acid-base titrations were used to characterize binding of Cu^{+2} and H^+ by the exudate ligands. Batch experiments in binary and ternary systems were conducted to evaluate the effect of the exudate ligands on Cu^{+2} sorption by the cells. Surface complexation modeling was performed to provide insights into the processes occurring.

2. Methods

2.1. Materials

All solutions were made from analytical grade reagents and 18 MΩ cm water. Solutions used in the experiments containing bacteria were sterilized by autoclaving or filtration through sterile 0.2 μm Sartorius Minisart cellulose acetate membrane filters. Laboratory glassware was autoclaved (121 °C for 20 min) and plasticware was purchased sterile.

Anoxybacillus flavithermus was isolated from the main wastewater drain at the Wairakei Geothermal Power Station (Wairakei, North Island, New Zealand) as previously described (Burnett et al., 2006b). Bacterial growth protocols were taken from Burnett et al. (2006a). Briefly the bacteria were pre-cultured in 5-mL volumes of trypticase soy broth (Becton, Dickinson and Company, USA). After growing for 24 ± 0.1 h at 60 °C, two of the 5-mL precultures were transferred to a 1-L volume of the trypticase soy broth which was placed in an orbital mixer incubator (100 rpm) at 60 °C for 24 ± 0.1 h, at which time the cells were in late stationary phase. Bacterial cells were removed from the growth medium by centrifugation (8230g, 15 min) and rinsed by three cycles of resuspending the cells by vigorous shaking in 0.01 M $NaNO_3$, centrifugation (8230g, 15 min) and discarding of the supernatant. After the final rinse the bacterial pellet was resuspended in 0.01 M $NaNO_3$ to yield the desired biomass concentration. All biomass concentrations are expressed as gL^{-1} dry weight of bacteria using a wet:dry ratio of 6.7:1 (Burnett et al., 2006a). This growth and rinsing protocol removes metals or exudates that may have been present in the growth medium and has been shown to leave the cells intact but metabolically inactive. Use of this growth protocol also ensures that the results from this study can be compared to results from previous studies by our group.

Solutions containing exudate ligands were prepared by culturing the bacteria as described above, resuspending the cells in 0.01 M $NaNO_3$ for a given period, and then removing the cells by centrifugation (8230g, 15 min) which for the purposes of this study is considered as differentiating the solution and particulate phases. One culture of bacteria was used to explore exudate production and reactivity towards Cu^{+2} over time. For this experiment *A. flavithermus* cells were suspended in

120 0.01 M $NaNO_3$ at pH 5.2 with a biomass concentration of 0.44 g L^{-1}, and exudate samples collected
121 over time between 1 and 70 h. These exudate solutions are termed EX*n* where *n* is the sampling
122 time in hours. A second culture of bacteria was prepared similarly but with a biomass concentration
123 of 5 g L^{-1}. The cells were removed from this suspension after 12 h in order to provide a single more
124 concentrated exudate solution, termed EXA.

125 *2.2. Polarography*

126 Differential pulse polarograms were recorded using a Metrohm VA Computrace with a static
127 mercury drop electrode. The following settings were used for the polarography: voltage step = 5 mV
128 with a step time of 1 s, pulse amplitude = 50 mV, and pulse time = 40 ms. All polarography
129 experiments were performed in 0.01 M $NaNO_3$ with the pH maintained at 5.2 using the non-
130 coordinating buffer 2-(N-morpholino)ethanesulfonic acid (MES). A pH of 5.2 was selected to
131 maximise Cu-ligand complexation while avoiding precipitation of copper hydroxides or carbonates,
132 which could occur at pH $\approx$ 6.5 under the conditions of our experiments. While some non-
133 coordinating buffers can participate in redox reaction under some conditions (Grady et al., 1988),
134 under the conditions of this study there was no change in the free Cu^{+2} polarographic response after
135 addition of MES (data not shown). The system was calibrated by addition of aliquots of Cu^{+2} (0.787
136 mM at pH 5.2) to a solution of 0.01 M $NaNO_3$ and MES buffer at pH 5.2 that had been sparged with
137 N_2 for 5 min. Aliquots of a given exudate solution were added to the solution of Cu^{+2} in 0.01 M
138 $NaNO_3$/MES. Changes in the polarograms as a function of added exudate solution were interpreted
139 in terms of extent of Cu^{+2}-ligand complexation. In addition experiments were also performed in
140 which Cu^{+2} was added to the exudate solutions, rather than the other way around. For comparison
141 and validation of the methodology, polarograms were recorded when 0.1 M potassium hydrogen
142 phthalate at pH 5.2 was added to Cu^{+2} in 0.01 M $NaNO_3$.

143 *2.3. Acid-Base Titrations*

144 The exudate solutions were acidified to pH $\approx$ 2.5, sparged with N_2 and titrated under a N_2
145 atmosphere with 0.01 M NaOH that had been prepared by diluting 50:50 (w/w) NaOH:water with N_2
146 sparged H_2O. A Metrohm 716 titrino autotitrator was used with the following settings: measuring

147 point density = 1, minimum increment = 1 μL, signal drift = 30 mV min^{-1} and equilibration time =
148 32 s. The electrode was calibrated by titrating 0.01 M $NaNO_3$ with 0.01 M NaOH and plotting the
149 measured pH as a function of the –log (H^+) added, where (H^+) is the molar concentration of H^+. For
150 data with pH < 7.0, the added (H^+) was calculated directly from the volume of NaOH added from the
151 endpoint. When the pH > 7, the added (H^+) was calculated from the (OH^-) added from the endpoint
152 using $(H^+) = 10^{-14}(OH^-)^{-1}(\gamma_1)^{-2}$ where γ_1 is the activity coefficient for a singly charged species
153 calculated from the Davies equation.

154 *2.4. Copper sorption experiments*

155 Copper sorption onto bacterial cells was measured using a batch method under an air atmosphere.
156 Suspensions of freshly rinsed *A. flavithermus* cells were suspended in various proportions of 0.01 M
157 $NaNO_3$ and EXA to give a biomass concentration of 0.044 gL^{-1} in solutions that had 0, 10, 30 or 90 %
158 EXA by volume. Fresh cells were combined with EXA because Cu^{+2} binding by either fresh cells or
159 EXA were determined in the experiments with binary system. The pH of the suspension was
160 lowered to ≈ 3.5, Cu^{+2} was added (4.7 μM), and aliquots were taken as the pH was raised in steps
161 of 0.5. The aliquots were equilibrated on an end-over-end mixer for 2 h then the pH was re-
162 measured and the bacteria were removed by centrifugation (8230g, 15 min). The supernatant was
163 removed, acidified to pH ≈ 2 and then the total Cu^{+2} concentration in solution, denoted Cu_{sol}, was
164 measured by inductively coupled plasma optical emission spectroscopy (ICP OES).

165 *2.5. Numerical modeling*

166 All modeling in this study was undertaken as described by Burnett et al. (2007) using FITMOD, a
167 modified version of the computer program FITEQL (Herbelin and Westall, 1996). The exudate
168 titration curves were modeled using the same discrete-site model as Seders and Fein (2011) using 1,
169 2 or 3 reactions of the form $L_iH \Leftrightarrow L_i^- + H^+$ where L_i refers to a specific ligand type. The goodness
170 of fit was assessed using the Weighted Sum of Squares divided by the Degrees of Freedom
171 (WSOS/DF) as previously described (Song et al., 2008). The relative uncertainty value for TOTH
172 was 0.02 and the absolute uncertainty in TOTH was 2×10^{-7}, i.e. 2 % of the smallest absolute value
173 of TOTH. The relative uncertainty in $\log(H^+)$ was 0.05. Modeling of the acid-base titration curves

174 was based on the solution (H^+), from the electrode response, as a function of the total H^+
175 concentration in the system, termed TOTH. For the blank titration, TOTH is known to be 0 M at the
176 titration endpoint. However, for the titration of the exudate solution there is no point when TOTH is
177 known. One solution is to assume that at some low pH all the ligands are protonated so TOTH =
178 (H^+). However, because the titration curve is very flat at low pH, using this approach causes a small
179 uncertainty in pH to correspond to a large uncertainty in TOTH. In this work, TOTH was optimized
180 from a starting value calculated from the (H^+) at the lowest pH in the titration.

181 Modeling of Cu^{+2}-ligand complexation was undertaken using the polarography data to estimate the
182 free Cu^{+2} concentration, denoted [Cu^{+2}], for systems over a range of total Cu^{+2} concentrations,
183 denoted TOTCu. Modeling Cu^{+2} binding by a ligand requires knowledge or assumptions of the
184 ligand pK_A's and the number of protons displaced when Cu^{+2} binds to the ligand. However, because
185 the polarography data was all collected at pH 5.2 the H^+ stoichiometry coefficient and the ligand pK_A
186 values will influence the logK for Cu^{+2} binding by a constant factor. Two different sets of
187 assumptions were made. In the first approach, modeling of Cu^{+2} binding by EX*n* was performed
188 assuming the same ligand pK_A values and H^+ stoichiometry coefficient as phthalate binding of Cu^{+2}.
189 This allows for a direct comparison between the Cu^{+2}-ligand logK values and the different effect of
190 exudate and phthalate on the Cu^{+2} polarography. In the second approach, modeling of Cu^{+2} binding
191 by EX*n* was undertaken assuming the reaction $HL + Cu^{+2} \Leftrightarrow LCu^+ + H^+$ and ligand pK_A value of
192 4.95. This modeling approach allows for a comparison between Cu^{+2} binding by the *A. flavithermus*
193 exudate and the *A. flavithermus* cells as reported by Burnett et al. (2007).

194 The modeling of proton and Cu^{+2} binding by the bacterial cell walls used the Donnan model, in
195 which the charge associated with sorption to cell walls is located within a certain volume that
196 accounts for the ion-penetrable layers of ionizable functional groups on the bacterial surface. The
197 approach was based on Burnett et al. (2007) who modelled Cu^{+2} and H^+ sorption using three surface
198 sites (R_1H^0, R_2H^0 and R_3H^+) with two sorbed Cu^{+2} species (R_1Cu^+ and R_1CuOH^0). Because the pH
199 range and TOTCu were both lower in our study we added a bacterial surface site, termed R_0H^0, with
200 a pK_A of 3 and a concentration of 1.34×10^{-4} mol g^{-1} as proposed in Burnett et al. (2006b). The

201 pK_A's and site concentrations were reoptimized from the Burnett et al. (2006b) titration data.
202 Sorption of Cu^{+2} was then modelled using the species R_nCu^{x+1} on the sites for n = 0 - 3 and, because
203 the data of this work are limited to pH < 6, sorption of $CuOH^+$ was not included in the modelling.
204 The bacteria surface area and Donnan volume were the same as used by Burnett et al. (2006b).

205 **3. Results**

206 *3.1. Polarography*

207 Polarograms measured for Cu^{+2} in 0.01 M $NaNO_3$ with MES at pH 5.2 and in the absence of
208 coordinating ligands had a free Cu^{+2} reduction peak, termed $(E_{1/2})_s$, at 0.089 V. The area of this peak
209 was proportional to the concentration of free Cu^{+2} ions. Figure 1a displays the polarograms that
210 were recorded as aliquots of EXA were sequentially added to 3.9 μM Cu^{+2} in 0.01 M $NaNO_3$ at pH
211 5.2. The height of the free Cu^{+2} peak decreased after the addition of just 100 μL of the EXA
212 solution, and continued to decrease as more of the EXA solution was added. The decreasing size of
213 the free Cu^{+2} peak indicates an increasing proportion of complexed Cu^{+2}, to the point that the free
214 Cu^{+2} is not detectable after 1.8 mL of EXA had been added. Incremental addition of the EXA
215 solution also caused the main Cu^{+2} peak to shift slightly from 0.089 to 0.064 V and led to the
216 appearance and growth of a second smaller peak at a potential, termed $(E_{1/2})_c$, of -0.13 V, which
217 indicated the presence of complexed Cu^{+2}. If the pH of the EXA-Cu^{+2} solution is lowered then the
218 free Cu^{+2} peak increased demonstrating that the complexation reaction was reversible (data not
219 shown). For comparison with the EXA, Figure 1b displays the polarograms that were recorded as
220 phthalate (L_p^{-2}) was added to 3.5 μM Cu^{+2} in 0.01 M $NaNO_3$ at pH 5.2. In contrast to the EXA
221 system, the addition of L_p^{-2} caused the free Cu^{+2} peak to shift gradually from 0.086 to 0.046 V, but
222 the peak height did not decrease.

223 Polarograms were measured after sequential addition of Cu^{+2} to undiluted exudates for all EX*n*
224 samples and the results for EX72 and EX2 are shown in Figures 2 and 3 respectively. For EX72 a
225 peak at -0.14 V was identifiable after 1.5 μM Cu^{+2} had been added to EX72 but no free Cu^{+2} peak
226 was observed. With addition of 3.1 μM Cu^{+2} the peak at -0.14 V increased in size and developed a
227 shoulder at -0.08 V. This shoulder grew and shifted to more positive potential to become the main

feature after addition of 6.9 μM Cu^{+2}. With addition of 14.4 μM Cu^{+2}, the main polarographic peak was at +0.06 V, close to the position of the free Cu^{+2} peak, but the area of this peak was only 11% of the area observed for the equivalent concentration of Cu^{+2} in 0.01 M $NaNO_3$. With 1.5 μM of Cu^{+2} added to EX2, free and complexed Cu^{+2} peaks were present at 0.08 and -0.13 V respectively, and only the free Cu^{+2} peak grew on subsequent Cu^{+2} addition.

Polarograms measured after sequential addition of Cu^{+2} to undiluted exudates from all EX*n* samples revealed increasing complexation capacity over time (i.e. *n*). Integrating the high potential peak in each polarogram provided an estimate of the free Cu^{+2}, which can then be expressed as the percentage of Cu^{+2} complexed as a function of TOTCu, where the complexed Cu^{+2} was taken as the difference between TOTCu and free Cu^{+2}. For each EX*n*, the percentage of complexed Cu^{+2} decreased as TOTCu increased, and the position of this line moved to higher TOTCu as *n* increased (Figure 4). For example after aging 0.44 gL^{-1} *A. flavithermus* for only 1 h in 0.01 M $NaNO_3$ the exudate ligands produced (EX1) were able to complex 60 % of the Cu^{+2} at a TOTCu of 1 μM. After aging for 72h (EX72), the exudate ligands complexed 60 % of the Cu^{+2} at a TOTCu of ≈ 35 μM (2,200 μgL^{-1}). In comparison, the EXA solution was collected, after 12 h, from a bacterial suspension that had ≈10 times the biomass concentration used for the EX*n* series and this exudate complexed 60 % of the total added Cu^{+2} at ≈ 0.1 mM TOTCu. In summary Cu^{+2} complexation by bacterial exudates became more significant as TOTCu decreased, the length of time bacteria are in the electrolyte increased or the amount of bacteria in the electrolyte increased.

3.2. Acid base titration curves

Figure 5 shows a typical acid base titration curve for EX72, which is plotted alongside modeled curves for *B. subtilis* exudate (Seders and Fein, 2011) and 0.44 gL^{-1} of *A. flavithermus* cells (Burnett et al., 2006b). The EX72 titration curve was not as steep as the 0.01 M $NaNO_3$ electrolyte blank. The amounts of NaOH required to raise the pH from 3.0 to 10.5 for the exudate and the electrolyte blank were 2.6 and 1.4 mM respectively, indicating a buffering capacity of 1.2 mM. The *A. flavithermus* bacterial cells required 1.8 mM OH^- to raise the pH from 3.0 to 10.5, corresponding to a

254 buffering capacity of 0.4 mM for the 0.44 gL^{-1} of cells. Therefore after 72 h the exudate had 3 times
255 higher number of deprotonatable groups than the bacterial cells.

256 Seders and Fein (2011) studied exudates from the Gram positive *B. subtilis* and the Gram negative
257 *S. oneidensis*. The exudates were obtained after the bacteria had been suspended in electrolyte for
258 2.5 h and similar titration curves were obtained for exudates from both bacterial species. The
259 buffering capacities of the Seders and Fein (2011) exudates was approximately 10 times less than
260 that of the bacterial cells. The greater buffering capacity of the *A. flavithermus* EX72 exudate than
261 the cells in our study is presumably due to the bacteria being in suspension for 72 h rather than the
262 2.5 h of Seders and Fein (2011). However many factors can influence exudate concentration. For
263 example Seders and Fein (2011) found that increasing the ionic strength from 0.01 to of 0.3 M
264 caused the exudate total site concentration to increase by a factor of 4 for *B. subtilis* but caused a
265 decrease by a factor of ≈ 4 for *S. oneidensis*.

266 *3.3. The Cu^{+2}-Exudate-Bacteria ternary system*

267 Copper sorption by *A. favithermus* cells in the presence of increasing proportions of EXA in the
268 system is shown in Figure 6 with the model results discussed in Section 4.4. At pH > 5 the Cu^{+2} in
269 solution, Cu_{sol}, increased with the proportion of EXA present as expected from the competition for
270 Cu^{+2} between the solution phase exudate ligands and the bacterial surface. For example at pH 6.5
271 the Cu_{sol} was 6 times greater in the system with 90% EXA compared to the electrolyte without EXA.
272 The opposite effect was observed at pH < 5, where Cu_{sol} decreased as the proportion of EXA
273 increased. In general, as the EXA concentration increased the relationship between Cu_{sol} and pH
274 became increasingly shallow. With 90 % EXA, Cu_{sol} was almost independent of pH with even a
275 slight positive slope between pH 4 and 5. While the increase in Cu_{sol} with increasing pH was small
276 in this study, it was the same phenomenon as observed by Gorman-Lewis et al. (2013) who found
277 that increasing pH caused a decrease in sorption of Np(V) by *B. subtilis* endospores when
278 complexing organic ligands were present in the aqueous phase.

279 **4. Discussion**

280 *4.1. Polarography*

281 The polarograms revealed several aspects of Cu^{+2} binding by the exudate. The polarographic peak
282 height of a species is proportional to the root of the species' diffusion coefficient. For the Cu-L_p
283 system the peak heights are similar but the very small Cu-EXA peaks suggest a substantially
284 smaller diffusion coefficient and presumably a larger molecular species. The position of the Cu-
285 EXA polarographic peak was informative. In general a free metal has a more positive $E_{1/2}$ than a
286 ligand complexed metal and $(E_{1/2})_c$ becomes increasingly negative for Cu^{+2} in complexes with
287 larger formation constants. This is reflected in the Lingane equation which relates $(E_{1/2})_c$ for a for
288 a CuL_j^{m+} complex to the formation constant (K), the ligand activity, (L), and the ligand
289 stoichiometry coefficient *j*. The Lingane equation is shown in Equation 1 where R, T, n and F have
290 their usual meanings and $\Delta E_{1/2}$ is the difference between the complexed Cu^{+2} and free Cu^{+2}
291 reduction peak positions. This behavior is subject to a number of assumptions relating to
292 electrochemical reversibility and equality of diffusion coefficients of free and complexed Cu^{+2} and
293 its application to trace metal aquatic chemistry has been discussed in Ernst et al. (1975).

294 $$\Delta E_{1/2} = (E_{1/2})_S - (E_{1/2})_C = \frac{RT}{nF} \ln K + j\frac{RT}{nF} \ln(L) \qquad \text{Eq. 1}$$

295 The polarograms from the Cu-L_p^{-2} and Cu-EXA systems revealed differences relative to the
296 expectations based on the Lingane Equation. Under the conditions of this study with Cu-L_p^{-2} the
297 uncharged complex CuL_p accounts for > 98% of all complexed copper and, as predicted by the
298 Lingane equation, $\Delta E_{1/2}$ increases linearly as a function of $\log[L_p^{-2}]$. In contrast, $\Delta E_{1/2}$ in the Cu-
299 EXA system did not follow the Lingane equation. In addition the relative peak heights of the free
300 and complexed Cu^{+2} showed that at least one assumption of the Lingane equation was not met in
301 the Cu-EXA system.

302 The $\Delta E_{1/2}$ for Cu^{+2} in the presence of EXA (0.22 V) was substantially larger than $\Delta E_{1/2}$ for Cu^{+2}-
303 L_P^{-2} system. For comparison, Croot et al. (1999) observed $\Delta E_{1/2}$ values up to 1.05 V for Cu^{+2} for a
304 range of complexing ligands found in sea water including exudates from a cyanobacterium, a
305 dinoflagellate and a diatom species. The $\Delta E_{1/2}$ values measured by Croot et al. (1999) suggested

these organisms exuded specialized Cu^{+2} binding ligands with logK values of up to 36. A slope of 0.039 was reported for the relationship between $\Delta E_{1/2}$ and logK for these ligands and this is in good agreement with the theoretical slope of 0.029 expected from Croot et al.'s (1999) simplified version of the Lingane Equation. Thus the $\Delta E_{1/2}$ values observed in our study suggest that value of K for the Cu-EXA complex was several orders of magnitude larger than that for CuL_P but also several orders of magnitude smaller than the specialized Cu^{+2} binding ligands identified by Croot et al. (1999). The value of logK for Cu^{+2} binding by the exudate is addressed specifically in Section 4.3.

The polarography of the EX*n* series demonstrated that more Cu^{+2} binding ligand was released in the exudate over the time the bacteria are in the electrolyte (Figure 4a and b). EX1 was the only sample that did not fit the relationship between aging time and exudate complexation capacity, in that it reproducibly displayed a slightly greater Cu^{+2} complex formation than EX2. This may have been a result of the procedures used to prepare the bacterial suspensions. After the final centrifuge rinse the bacteria were shaken fairly vigorously to resuspend them in the 0.01 M $NaNO_3$. This may have caused some disruption to the cell walls, releasing organic fragments that then reassociated with the cell wall over the first two hours of the comparatively gentle mixing during the EX*n* suspension aging. In general it is clear from Figure 4a that in bacterial systems the significance of Cu^{+2} complexation by exudate increases as the suspension ages but also increases as the total Cu^{+2} concentration decreases.

4.2. Titrations

The EX72 titration curves were modeled using the same discrete-site model as Seders and Fein (2011) and the model output with 1, 2 or 3 reactions of the form $L_iH \Leftrightarrow L_i^- + H^+$ are presented in Table 1. The EX72 titration curve was reasonably well described using a 2 site model with a WSOS/DF of 1.6. This compares to the average WSOS/DF value of 73 from the 2 site model approach applied by Seders and Fein (2011). The much higher WSOS/DF of Seders and Fein (2011) presumably reflects the greater inflection in the titration curve around pH 7 (which is not described with the 2 site model), but the WSOS/DF is also highly dependent on the input uncertainty values

used in FITEQL which were not reported in Seders and Fein (2011). The WSOS/DF is often used to determine the acceptability of a model approach but for this to be meaningful requires that realistic values for uncertainties are used. The uncertainties used for the values in Table 1 are given in Section 2.5 and are based on the method previously described (Dzombak and Morel, 1990) with an uncertainty estimate of 2 %. If the uncertainties input to FITMOD were based on estimates of 0.5 or 5 % then WSOS/DF values of 45.8 and 0.45 respectively are obtained from the 2 site model fit. Adding a third site to the model allowed improved fitting of the inflection in the EX72 titration curve at $\approx$ pH 7 but, because this feature was fairly subtle, the uncertainties in the [HL] and pK_A for this site were comparatively high.

The three site model pK_A values for the *A. flavithermus* exudate were very similar to the Seders and Fein (2011) pK_A values for exudates from both the Gram positive bacteria *B. subtilis* (Table 1) and from the Gram negative *S. oneidensis* (3.9 ±0.3, 6.6±0.4 and 9.3±0.1). The similarity in pK_A values is particularly significant because Seders and Fein (2011) proposed a 'universal' soluble fraction associated with bacterial exudate. This proposal was based on the similar pK_A's of exudates from the Gram positive and Gram negative bacteria as well as similar FTIR spectra for these exudates. The Seders and Fein (2011) exudate FTIR spectra had bands attributed to proteins and polysaccharides and were also considered to be similar to the FTIR of bacterial cell wall fragments apart from the exudate spectra having more intense polysaccharide bands.

A "universal exudate" is analogous to the proposed "universal" set of pK_A's and site concentrations that have been used to characterize proton and cation binding by many bacterial cells (Borrok et al., 2004). The *A. flavithermus* exudate pK_A's in our study further support the idea of a "universal exudate". The apparent generic nature of bacterial exudates and their significant Cu^{+2} complexation justifies studies to characterize the molecular size distribution and functional groups of the exudate ligands. This was beyond the scope of the current study which focused on quantifying the significance of the exudates. Similarly Seders and Fein (2011) employed a general definition of an exudate and stated that exudates probably contain components arising from both cell lysis and passive excretion.

360 *4.3. Modeling Cu^{+2} binding by the A. flavithermus cells and exudates*

361 Proton and Cu^{+2} sorption by *A. flavithermus* cells was modelled using 4 site types, R_0H^0, R_1H^0,
362 R_2H^0 and R_3H^+ as discussed in Section 2.5. A 4 site approach has been used in many previous
363 studies to describe the shape of pH sorption edges for bacterial cells, which are less steep then pH
364 sorption edges of cations on iron oxides (Borrok et al., 2004; Song et al., 2009). Table 2 gives the
365 optimized parameters for proton binding and Cu^{+2} binding to the 4 sorption sites on the *A.*
366 *flavithermus* cells that were optimized in this work from titrations in Burnett et al. (2006a) and Cu^{+2}
367 sorption from (Burnett et al., 2007) and this study. Figure 7 gives the Cu^{+2} sorption data used for
368 optimization with the model fit to the data with the parameters in Table 2.

369 Prior to modelling Cu^{+2} binding by the exudate it is useful to note the number of Cu^{+2} binding
370 ligands of EX72 ($\approx$ 50 μM g^{-1} from Figure 4a) was a small fraction of the EX72 H^+ binding ligands
371 which ranged from 0.21 to 2.24 mmol g^{-1}. Therefore in each exudate sample the concentration of
372 Cu^{+2} binding ligands was determined with the logK for complex formation by modeling the
373 relationship between the measured free Cu^{+2} and TOTCu with FITMOD. Table 3 shows the
374 FITMOD output using an "H_2L model" with the reaction $H_2L+Cu^{+2} \Leftrightarrow Cu\text{-}L + 2H^+$ and the ligand
375 pK_A values were the same as phthallic acid. The optimized Cu^{+2}-ligand logK values had a weighted
376 average and 95 % confidence interval of -1.37 $\pm$ 0.10 (Table 3). The optimized [H_2L] values
377 increased over time and are shown with the data in Figure 4b. Model predictions of the %
378 complexed Cu^{+2} versus TOTCu based on these Cu^{+2} complexation parameters are shown in Figure
379 4a and provide a good description of the experimental data, especially given the simplicity of the
380 model and the potential complexity of the system. The logK for forming the neutral CuL_p complex
381 by the analogous reaction is -4.34 (Gustafsson, 2006) so the exudate complex logK is 3.0 log units
382 larger than that of phthalate when both reactions are expressed using the same stoichiometry. As
383 previously discussed, Croot et al.'s (1999) simplified version of the Lingane Equation has a
384 theoretical slope of 0.029 (i.e. 2.303RT/2F) relating logK to $\Delta E_{1/2}$ and a measured slope of 0.039 for
385 a range of seawater ligands. In comparison, in this study we obtain a comparable slope of 0.043

386 based on the weighted average logK of -1.37 for the Cu-exudate complex and using the $\Delta E_{1/2}$
387 calculated for phthalate at 1 M.

388 The second approach to modeling Cu^{+2} binding by EX*n* used an HL model with the reaction HL +
389 $Cu^{+2} \Leftrightarrow LCu^{+} + H^{+}$ and a ligand pK_A value of 4.95. This modeling approach allows for a comparison
390 between Cu^{+2} binding by the *A. flavithermus* exudate and the *A. flavithermus* cells as reported by
391 Burnett et al. (2007). With this model framework, the optimized Cu^{+2}-exudate logK value had a
392 weighted average and 95 % confidence interval of 1.80 ± 0.10. For comparison, Burnett et al. (2007)
393 reported a logK of -0.91 for Cu^{+2} binding by R_1H^0 sites on the cell wall, indicating that the exudate
394 binds Cu^{+2} substantially more strongly than the cell wall.

395 *4.4. Modeling Cu^{+2} binding by the A. flavithermus cells in systems with exudate*

396 It is clear that there is no mechanism evident from the binary systems that can account for the
397 observed decrease in Cu_{sol} in the presence of EXA at pH < 5. This observation must indicate some
398 additional process occurring in the ternary system that is not evident from the binary systems. To
399 investigate the significance of the additional process the ternary systems were modelled using the
400 parameters derived from the binary systems. This modeling used the H_2L model for the Cu-exudate
401 complex (Table 3) with the $[H_2L]$ calculated from the EXA value in Table 3 multiplied by the
402 proportion of EXA present in the system. In addition this modeling used the logKs for Cu^{+2} sorption
403 by the bacteria that were optimized from the dataset with 4.7 μM TOTCu (1.18 and -0.88 for R_0Cu^{+}
404 and R_3Cu^{+2} respectively). The model output predicted that the Cu_{sol} would increase with higher
405 $[H_2L]$ as expected, but the extent of this increase was substantially greater than the data (Figure 6).
406 Moreover, while it was expected that the modeled Cu_{sol} would be greater than the measured Cu_{sol} at
407 pH < 5, this was in fact true over the entire pH range. The system was also modeled using the HL
408 exudate model and the result was very similar.

409 The observed effect of the exudate on Cu^{+2} sorption by the cells was quite distinct from the effect
410 of L_p^{-2} on Cd^{+2} sorption by *B. subtilis* where the presence of L_p^{-2} decreases Cd^{+2} sorption over the
411 entire pH range of the sorption edge (Song et al., 2008). Furthermore the extent of the inhibition of
412 Cd^{+2} sorption by L_p^{-2} is correctly predicted using cation sorption constants derived from binary Cd^{+2}-

413 bacteria sorption experiments and the literature solution Cd^{+2}-phthalate complex logK values. This
414 indicated that with Cd^{+2}-phthalate-bacteria there are no chemical reactions occurring in the ternary
415 system that are not occurring in the binary system. In particular it is clear that there is no
416 appreciable interaction between the Cd-phthalate complexes and the cell wall surface.

417 For the Cu^{+2}-exudate-bacteria system a model based on the binary systems could fit the data from
418 the ternary systems. This indicates that there is a significant interaction between the three
419 components in the ternary system. The significance of this interaction would not have been evident
420 without an incremental approach and the modeling of the binary systems. The difference between
421 the binary model result and the data for the system with 90 % EXA did not change much with pH
422 suggesting that the ternary interaction was not strongly pH dependent. Two possible explanations
423 for the observed behavior are presented here but a full understanding of this system requires more
424 study.

425 One possible explanation for the observation is a hydrophobic interaction. For example, in the
426 absence of sorbing cations, bacterial cells are generally observed to take up ligands such as EDTA
427 and L_p^{-2} only at pH values at which they are neutrally charged and this has been attributed to a
428 hydrophobic interaction. If the LCu^0 complex is uncharged then it could be taken up by the cell
429 membrane via a similar mechanism. Many ligands are able to solubilize Cu^{+2} in nonpolar solvents
430 and are used in numerous liquid-liquid extraction procedures (Anthemidis and Ioannou, 2009).
431 There was no evidence of this type of hydrophobic interaction influencing the Cd^{+2}- L_p^{-2}-bacteria
432 system however, even under experimental conditions when up to 40 % of the Cd^{+2} was present as the
433 neutral CdL_p complex (Song et al., 2009). This was attributed to the organic fraction of the complex
434 being small and the positive charge on the Cu^{+2} being poorly screened by the single L_p^{-2} ligand.
435 However if the Cu-L complex with the exudate is larger than Cu-L_p (as suggested by the
436 polarography) and more hydrophobic then this could explain the observed Cu^{+2} partioning in the
437 ternary system.

438 A second possible interaction that could explain the observation is the formation of a ternary
439 complex. For example, Cu^{+2} could be present as a bridge between the exudate ligand and a bacterial

surface sorption site. This would be analogous to the way in which some ligands promote cation sorption onto iron oxide surfaces. For example, Boily et al. (2005) reported a ternary surface complex in which Cd^{+2} ions sorbed on the goethite surface are also coordinated to phthalate ions. In the study of Boily et al. (2005) both Cd^{+2} and phthalate sorption by goethite are enhanced in ternary systems compared to binary systems. There are a range of possible stoichiometries for a ternary complex reflecting the four types of bacterial surface sites and also different possible degrees of protonation (Equation 3):

$$H_2L + Cu^{+2} + R_nH \leftrightarrow R_nCuLH_{3-x}^{(2-x)+} + xH^+ \qquad Eq.3$$

The data from Figure 6 were modeled using the reactions from the binary model with the addition of one reaction for a ternary complex. The log K for the ternary complex was the only optimized parameter. The system was modeled using many different ternary complexes involving different cell wall surface sites and with different H^+ stoichiometry coefficients. In general the effect of adding any ternary complex to the model was to decrease the modeled Cu_{sol}. When the logK for formation of a ternary complex was optimized the model would over predict Cu_{sol} for some data points and under predict Cu_{sol} for other data points and the overall goodness of fit was dependent on the assumptions for the surface site involved and the H^+ stoichiometry of the reaction. The best fitting model invoked a ternary complex stoichiometry of R_2CuLH^0 and had an optimized logK of 3.60 for Equation 3 with a WSOS/DF of 5.7. This model provided a reasonable description of the effect of the exudate on Cu^{+2} sorption by the bacteria (Figure 8). This certainly does not suggest that this specific reaction is occurring but it does demonstrate that this type of reaction can account for the complex effect of exudate ligands on the behavior of Cu^{+2} in suspensions of *A. flavithermus* cells.

An important issue that arises from this study is the effect of bacterially exuded ligands on the many reported cation sorption studies by bacterial cells. This can be answered in the case of the data used in this study where the concentration of exuded ligands from *A. flavithermus* cells over two hours would be approximately 4 μM per g of bacteria. Therefore in the Cu^{+2} sorption data by cells in ostensibly binary systems (Figure 7) the mole ratio of ligand to Cu^{+2} concentrations ranged from

466 0.005 to 0.04. This was much lower than the ternary system data in Figure 6 where the mole ratio of
467 ligand to Cu^{+2} concentrations ranged from 1 to 11. Adding the exudate ligand concentrations and
468 Cu-L reactions to the model for the optimization of sorption constants in binary Cu-cell experiments
469 made almost no difference to the optimized sorption constants reported in Table 2 where the exudate
470 was ignored. However, it is clear that in experiments with high bacteria concentrations and low
471 metal concentrations the exudate will become increasingly significant.

472 **5. Conclusions**

473 The distribution of a trace metal between the solid and solution phase is clearly important for
474 predicting trace metal transport, fate and toxicity. Comparatively few investigations have focused
475 on systems containing a trace metal, a ligand and bacterial cells, even though bacteria are
476 ubiquitous in near-surface environments, their cell walls have high affinities for many trace metals,
477 and the cells naturally exude metal-complexing ligands via metabolism and cell lysis. This study
478 has evaluated the behavior of Cu^{+2} in the presence of exudate ligands produced by aging cells of
479 the bacterium *A. flavithermus* in 0.01 M $NaNO_3$ at pH 5.2. The Cu^{+2} binding of the exudate was
480 well described by the model reaction $H_2L + Cu^+ \Leftrightarrow LCu + 2H^+$ with logK = -1.37, assuming that the
481 ligand has the same pK_A values as phthalate. The modeling and polarography suggested that the
482 logK for the Cu^{+2}-ligand complex was several orders of magnitude larger than the logK for the
483 Cu^{+2}-phthalate complex but much smaller than the logKs inferred by Croot et al. (1999) for
484 specialized Cu^{+2} binding ligands produced by some seawater microorganisms.

485 This study has also evaluated the sorption of Cu^{+2} by bacterial cells in ternary systems
486 containing the exudate ligands. In general the presence of exudate enhanced Cu^{+2} sorption at pH <
487 5 and inhibited Cu^{+2} sorption at pH > 5. Across the whole pH range Cu^{+2} sorption was
488 substantially greater than expected from modelling based on the binary systems. This implies the
489 formation of a ternary surface complex where Cu^{+2} may act as a bridge between the exudate ligand
490 and a binding site on the bacterial surface. The experimental data from the ternary systems were
491 best described by the model reaction $R_2H^0 + Cu^{2+} + H_2L \Leftrightarrow R_2CuLH^0 + 2H^+$ with logK = 3.60. The

modeling demonstrated that a reaction of this type can account for the effect of the exudate ligands on Cu^{+2} behavior in the presence of *A. flavithermus* cells.

6. References

Albrecht-Gary, A.M., Crumbliss, A.L., 1998. Coordination chemistry of siderophores: Thermodynamics and kinetics of iron chelation and release. Metal Ions in Biological Systems, Vol 35 35, 239-327.

Ali, M.A., Dzombak, D.A., 1996. Interactions of copper, organic acids, and sulfate in goethite suspensions. Geochim. Cosmochim. Acta 60, 5045-5053.

Andrews, S.C., Robinson, A.K., Rodriguez-Quinones, F., 2003. Bacterial iron homeostasis. FEMS Microbiol. Rev. 27, 215-237.

Anthemidis, A.N., Ioannou, K.-I.G., 2009. Recent developments in homogeneous and dispersive liquid-liquid extraction for inorganic elements determination. A review. Talanta 80, 413-421.

Babechuk, M.G., Weisener, C.G., Fryer, B.J., Paktunc, D., Maunders, C., 2009. Microbial reduction of ferrous arsenate: Biogeochemical implications for arsenic mobilization. Applied Geochemistry 24, 2332-2341.

Boily, J.-F., Sjöberg, S., Persson, P., 2005. Structures and stabilities of Cd(II) and Cd(II)-phthalate complexes at the goethite-water interface. Geochim. Cosmochim. Acta 69, 3219-3235.

Borrok, D., Fein, J.B., Kulpa, C.F., 2004. Proton and Cd adsorption onto natural bacterial consortia: Testing universal adsorption behavior. Geochim. Cosmochim. Acta 68, 3231–3238.

Burnett, P.-G.G., Daughney, C.J., Peak, D., 2006a. Cd adsorption onto *Anoxybacillus flavithermus*: Surface complexation modeling and spectroscopic investigations. Geochim. Cosmochim. Acta 70, 5253–5269.

Burnett, P.G., Heinrich, H., Peak, D., Bremer, P.J., McQuillan, A.J., Daughney, C.J., 2006b. The effect of pH and ionic strength on proton adsorption by the thermophilic bacterium Anoxybacillus flavithermus. Geochim. Cosmochim. Acta 70, 1914-1927.

Burnett, P.G.G., Handley, K., Peak, D., Daughney, C.J., 2007. Divalent metal adsorption by the thermophile Anoxybacillus flavithermus in single and multi-metal systems. Chem. Geol. 244, 493-506.

Croot, P.L., Moffett, J.W., Luther, G.W., 1999. Polarographic determination of half-wave potentials for copper-organic complexes in seawater. Mar. Chem. 67, 219-232.

Daughney, C.J., Hetzer, A., Heinrich, H.T.M., Burnett, P.G.G., Weerts, M., Morgan, H., Bremer, P.J., McQuillan, A.J., 2010. Proton and cadmium adsorption by the archaeon Thermococcus zilligii: Generalising the contrast between thermophiles and mesophiles as sorbents. Chem. Geol. 273, 82-90.

Davis, J.A., Leckie, J.O., 1978. Effect of adsorbed complexing ligands on trace metal uptake by hydrous oxides. Environ. Sci. Technol. 12, 1309-1315.

Dogan, N.M., Kantar, C., Gulcan, S., Dodge, C.J., Yimaz, B.C., Mazmanci, M.A., 2011. Chromium(VI) Bioremoval by Pseudomonas Bacteria: Role of Microbial Exudates for Natural Attenuation and Biotreatment of Cr(VI) Contamination. Environmental Science & Technology 45, 2278-2285.

Dzombak, D.A., Morel, F.M.M., 1990. Surface Complexation Modeling: Hydrous Ferric Oxide. John Wiley & Sons, New York.

Ernst, R., Allen, H.E., Mancy, K.H., 1975. Characterization of trace-metal species and measurement of trace-metal stability-constants by electrochemical techniques. Water Res. 9, 969-979.

Fein, J.B., Delea, D., 1999. Experimental study of the effect of EDTA on Cd adsorption by *Bacillus subtilis*: a test of the chemical equilibrium approach. Chem. Geol. 161, 375-383.

Fujii, M., Imaoka, A., Yoshimura, C., Waite, T.D., 2014. Effects of Molecular Composition of Natural Organic Matter on Ferric Iron Complexation at Circumneutral pH. Environ. Sci. Technol. 48, 4414-4424.

Gorman-Lewis, D., Jensen, M.P., Harrold, Z.R., Hertel, M.R., 2013. Complexation of neptunium(V) with Bacillus subtilis endospore surfaces and their exudates. Chem. Geol. 341, 75-83.

Grady, J.K., Chasteen, N.D., Harris, D.C., 1988. Radicals from Goods buffers. Anal. Biochem. 173, 111-115.

Gustafsson, J.P., 2006. Visual MINTEQ, Version 2.51.

Heinrich, H.T.M., Bremer, P.J., Daughney, C.J., McQuillan, A.J., 2007. Acid-base titrations of functional groups on the surface of the thermophilic bacterium Anoxybacillus flavithermus: Comparing a chemical equilibrium model with ATR-IR spectroscopic data. Langmuir 23, 2731-2740.

Herbelin, A.L., Westall, J.C., 1996. FITEQL: A computer program for determination of chemical equilibrium constants from experimental data. Chemistry Department, Oregon State University, Corvallis, OR.

Jackson, B.P., Ranville, J.F., Neal, A.L., 2005. Application of flow field flow fractionation-ICPMS for the study of uranium binding in bacterial cell suspensions. Analytical Chemistry 77, 1393-1397.

Le Person, A., Moncomble, A., Cornard, J.-P., 2014. The Complexation of Al-III, Pb-II, and Cu-II Metal Ions by Esculetin: A Spectroscopic and Theoretical Approach. J. Phys. Chem. A 118, 2646-2655.

Lombardi, A.T., Hidalgo, T.M.R., Vieira, A.A.H., 2005. Copper complexing properties of dissolved organic materials exuded by the freshwater microalgae Scenedesmus acuminatus (Chlorophyceae). Chemosphere 60, 453-459.

Mason, R.P., 2013. Trace metals in aquatic systems, West Sussex, Wiley-Blackwell.

Nogueira, P.F.M., Lombardi, A.T., Nogueira, M.M., 2012. Cylindrospermopsis raciborskii exudate-Cu complexes: impact on copper dynamics and bioavailability in an aquatic food chain. Environmental Science and Pollution Research 19, 1245-1251.

Ohnuki, T., Yoshida, T., Ozaki, T., Kozai, N., Sakamoto, F., Nankawa, T., Suzuki, Y., Francis, A.J., 2007. Chemical speciation and association of plutonium with bacteria, kaolinite clay, and their mixture. Environmental Science & Technology 41, 3134-3139.

Saw, J.H., Mountain, B.W., Feng, L., Omelchenko, M.V., Hou, S., Saito, J.A., Stott, M.B., Li, D., Zhao, G., Wu, J., Galperin, M.Y., Koonin, E.V., Makarova, K.S., Wolf, Y.I., Rigden, D.J., Dunfield, P.F., Wang, L., Alam, M., 2008. Encapsulated in silica: genome, proteome and physiology of the thermophilic bacterium Anoxybacillus flavithermus WK1. Genome Biology 9.

Seders, L.A., Fein, J.B., 2011. Proton binding of bacterial exudates determined through potentiometric titrations. Chem. Geol. 285, 115-123.

Song, Y., Swedlund, P.J., Singhal, N., 2008. Copper(II) and Cadmium(II) Sorption onto Ferrihydrite in the Presence of Phthalic Acid: Some Properties of the Ternary Complex. Environ. Sci. Technol. 42, 4008-4013.

Song, Y.T., Swedlund*, P.J., Singhal, N., Swift, S., 2009. Cadmium(II) Speciation in Complex Aquatic Systems: A Study with Ferrihydrite, Bacteria, and an Organic Ligand. Environ. Sci. Technol. 43, 7430-7436.

Tipping, E., 2002. Cation binding by humic substances, Cambridge University Press, 2002, New York.

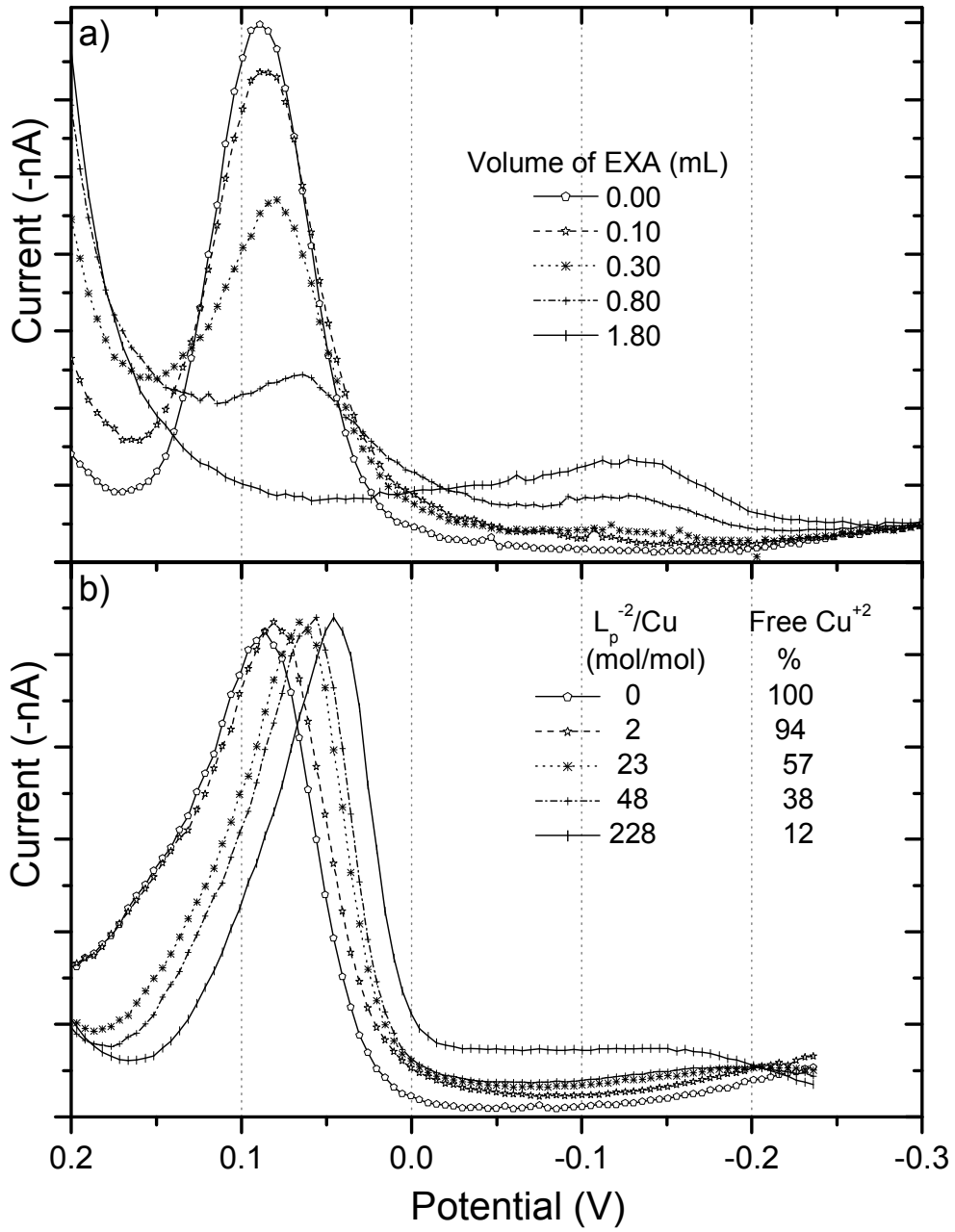

587

588 **Figure 1** Differential pulse polarograms for a) adding bacterial exudate solution EXA to 10 mL of 3.9
589 μM Cu^{+2} in 0.01 M $NaNO_3$ at pH 5.2. b) adding phthalate to 3.5 μM Cu^{+2} in 0.01 M $NaNO_3$ at pH 5.2,
590 where the legend shows the % of free Cu^{+2} calculated using parameters from Gustafsson (2006).

591

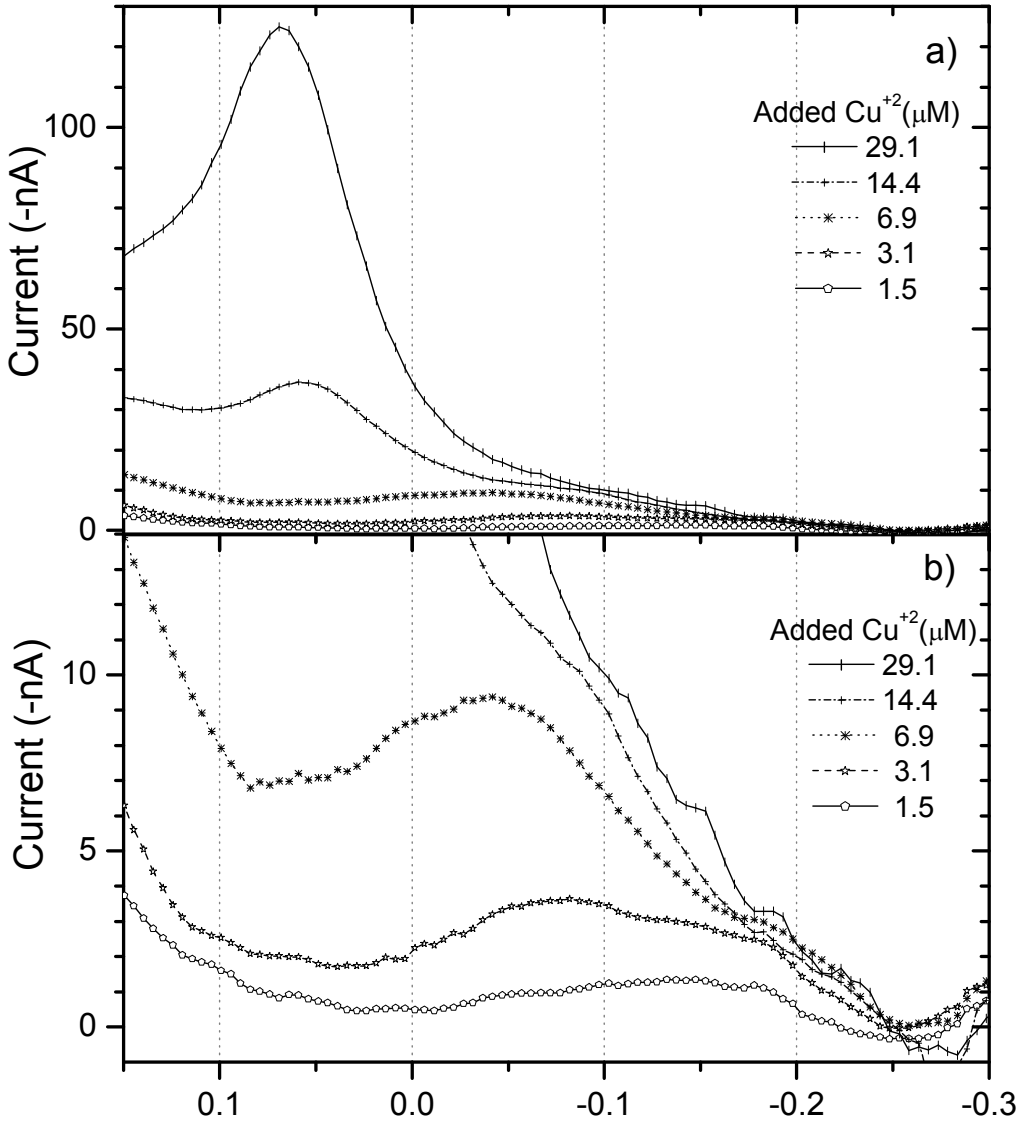

Figure 2 Differential pulse polarograms measured after Cu^{+2} was added to EX72 at pH 5.2. The total added Cu^{+2} concentration is given in the legend. b) as for a) but with an expanded y axis scale.

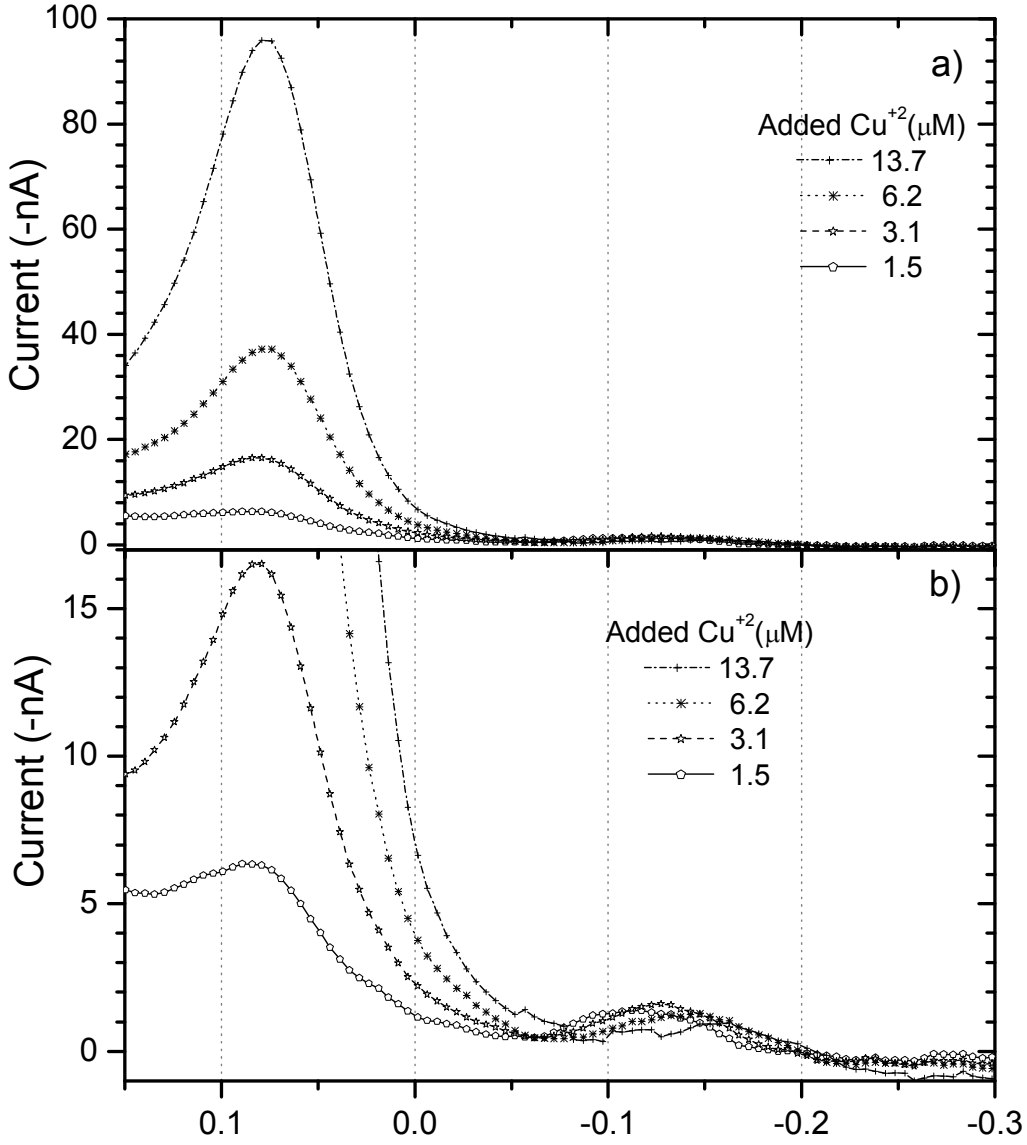

599

600 **Figure 3** Differential pulse polarograms measured after Cu^{+2} was added to EX2 at pH 5.2. The total

601 added Cu^{+2} concentration is given in the legend. b) as for a) but with an expanded y axis scale

602

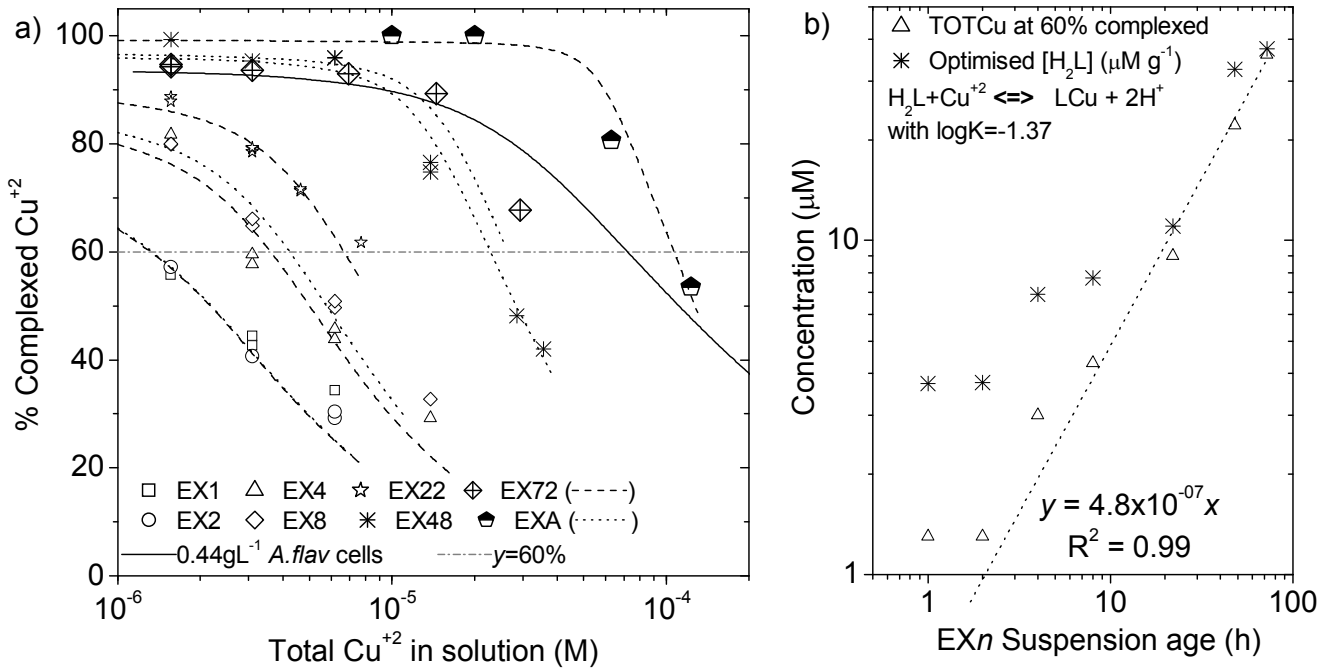

603

604 **Figure 4** a) Percent complexed Cu^{+2} at pH 5.2 in exudates extracted from *A. flavithermus* suspensions
605 for the EX*n* series and EXA. Points are data and lines are models (Section 4.3). The model is also
606 shown for 0.44 gL^{-1} *A. flavithermus* cells. b) The total [Cu^{+2}] where 60 % of the Cu^{+2} was complexed (Δ)
607 and the optimized site concentration (*) for the EXn series (determined with some extrapolation where
608 necessary).

609

610

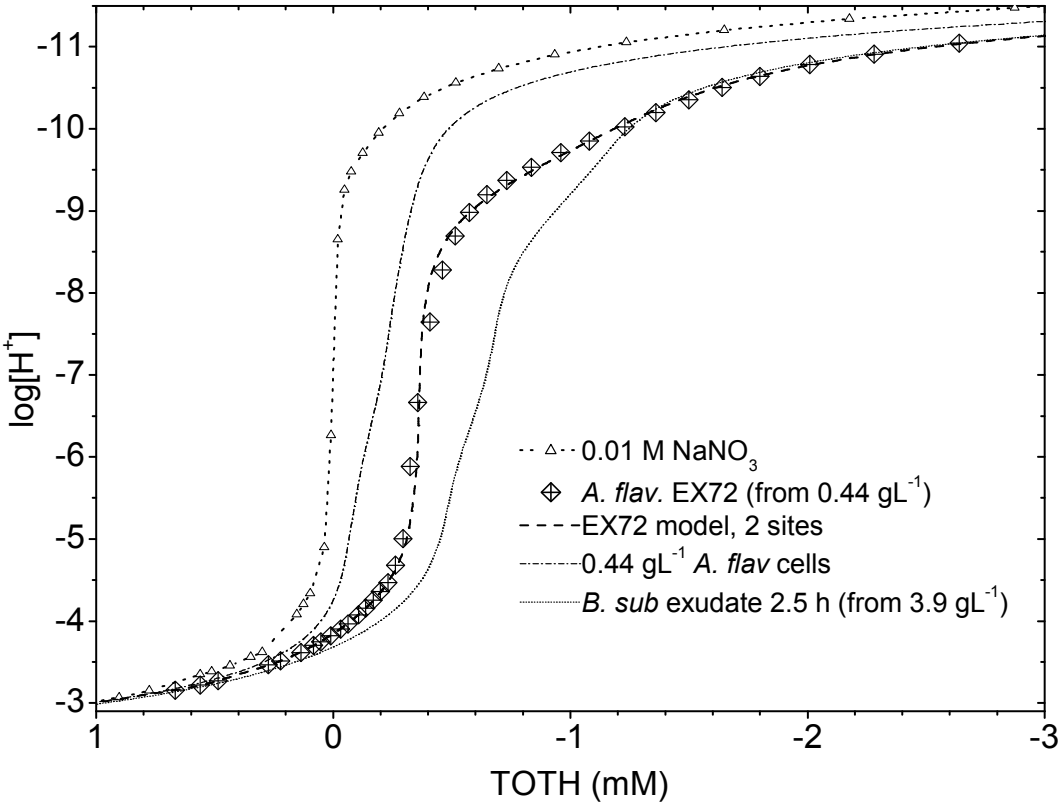

611

612 **Figure 5** Acid-base titration curve for *A. flavithermus* exudate (EX72) compared to *A. flavithermus*
613 cells (Burnett et al., 2007) and exudate from *B. subtilis* (Seders and Fein, 2011). Points are data, lines
614 are modelled.

615

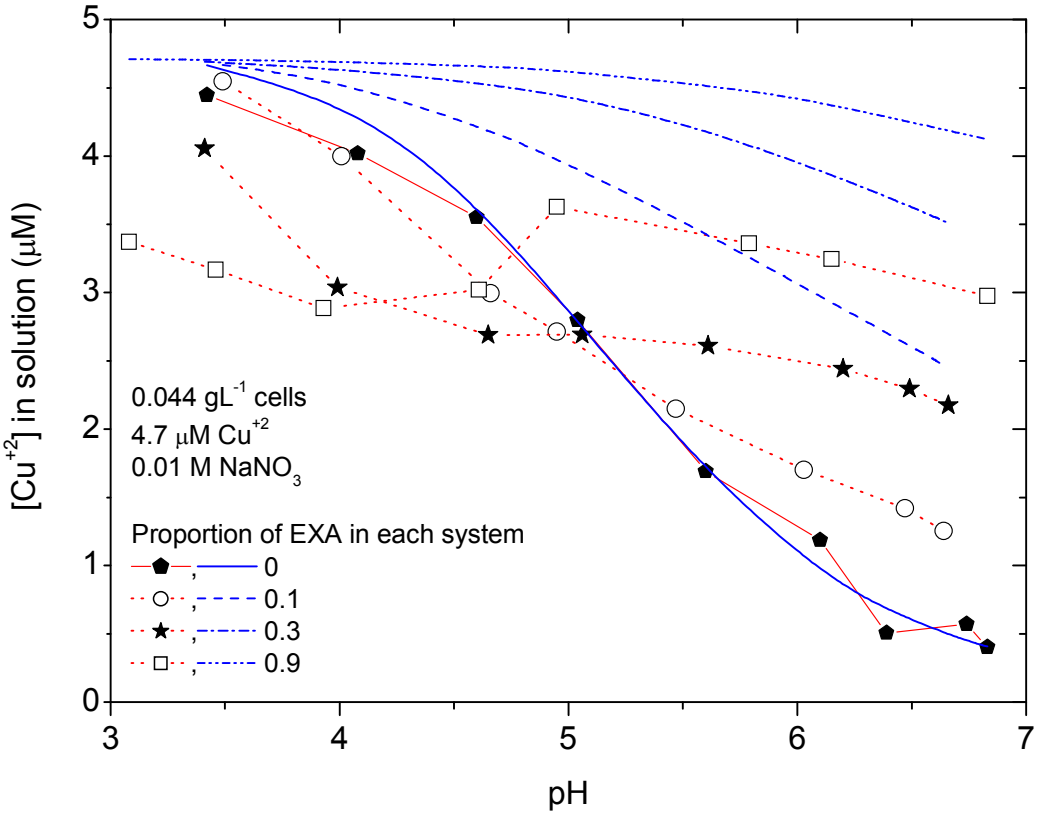

616
617 **Figure 6** Effect of *A. flavithermus* exudate (EXA) on Cu^{+2} sorption to bacterial cells. Points are data
618 (joined by red dotted lines to aid visualization), dashed blue lines are modelled with the parameters
619 from the binary systems (see text).

620

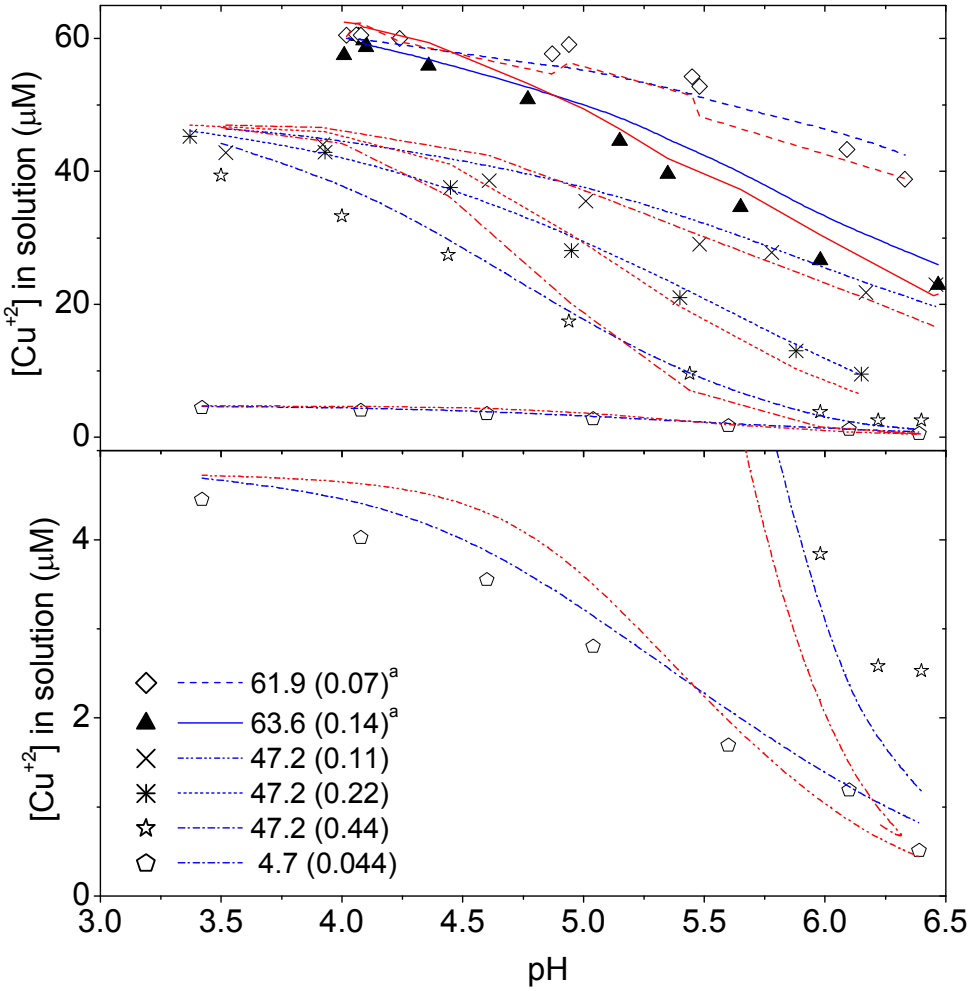

621

622 **Figure 7** The sorption of Cu^{+2} onto *A. flavithermus* as a function of pH (points are data, blue lines are
623 models based on Table 1 and red lines are models based on (Burnett et al., 2007). Legend shows
624 TOTCu in μM and dry weight of bacteria in gL^{-1}. Data marked [a] from Burnett et al. (2007) while other
625 data are from this work.

626

627

628

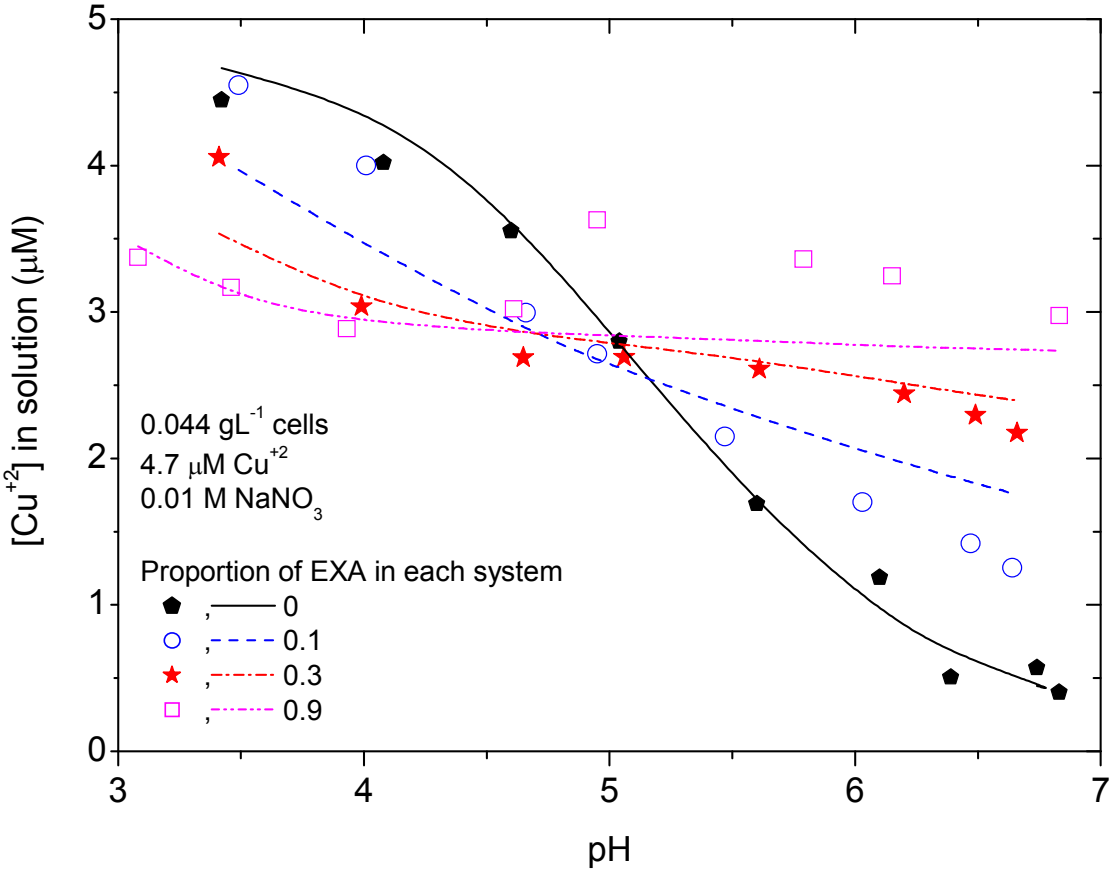

Figure 8 Effect of *A. flavithermus* exudate (EXA) on Cu^{+2} sorption to bacterial cells. Points are data and lines are modelled with the parameters from the binary system including the ternary complex R_2LCuLH^0.

637 **Table 1** Optimised parameters for the titration of *A. flavithermus* exudate after 72 h compared to *B.*
638 *subtilis* exudate after 2.5 h (Seders and Fein, 2011) and *A. flavithermus* cells (Burnett et al., 2006b).
639

Model	$[L_xH]$[a] (mmol g^{-1})	L_xH pK_A	WSOS/DF
1 monoprotic ligand	1.16 (0.01)	4.96 (0.02)	115
2 monoprotic ligands			
L_1H	0.86 (0.02)	4.12 (0.04)	1.56
L_2H	2.30 (0.05)	9.66 (0.03)	
3 monoprotic ligands			
L_1H	0.84 (0.03)	3.96 (0.05)	0.47
L_2H	0.21 (0.03)	7.10 (0.32)	
L_3H	2.24 (0.05)	9.78 (0.04)	
B. subtilis exudate			
L_1H	0.12 (0.06)	4.0 (0.3)	Range of
L_2H	0.05 (0.03)	6.6 (0.5)	6-10
L_3H	0.12 (0.04)	9.2 (0.1)	
A.flavithermus cells			
R_1H^0	0.533	4.94	
R_2H^0	0.179	6.85	
R_3H^+	0.142	7.85	

640

641 [a] Standard deviations in brackets are from FITMOD (this study) or the range of values obtained (Seders
642 and Fein, 2011)

643

644

645

646

Table 2 The H^+ and Cu^{+2} sorption parameters for *A. flavithermus* cells with standard deviations in parentheses.

Site	logK R_nH^{x-1}	μmol g^{-1}	logK R_nCu^{x+1}
R_0H^0	-3.00[a]	125[a]	1.01 (0.03)
R_1H^0	-4.54 (0.02)	459 (6)	No convergence
R_2H^0	-6.32 (0.05)	194 (5)	-2.29[b] (0.04)
R_3H^{+1}	-8.56 (0.07)	204 (2)	-2.25 (0.05)

[a] value was not optimized so there is no standard deviation

[b] determined with the logK values for R_0Cu^+ and R_3Cu^{+2} fixed at 1.01 and -2.25.

655

656 **Table 3** Optimised parameters logK and $[H_2L]$ for the reaction $H_2L + Cu^{+2} \Leftrightarrow LCu + 2H^+$ determined

657 from the polarography data (Figure 4a), assuming H_2L pK_A values are the same as phthallic acid.

658

659

EXn sample	$[H_2L]^a$ (μmol g^{-1})[c]	logK	$[H_2L]^b$ logK fixed (μmol g^{-1})	WSOS/DF[a]
1	6.7 (1.1)	-1.91 (0.11)	3.7 (0.1)	0.62
2	5.0 (0.6)	-1.71 (0.11)	3.8 (0.2)	0.98
4	6.7 (0.4)	-1.32 (0.07)	6.9 (0.2)	6.33
8	8.5 (0.4)	-1.47 (0.05)	7.7 (0.2)	3.94
22	10.9 (0.5)	-1.36 (0.04)	11 (0.2)	4.81
44	27.7 (0.7)	-1.12 (0.03)	32.5 (0.5)	13.5
72	52 (1.9)	-1.72 (0.03)	37.5 (0.7)	1.23
EXA	10.8 (0.2)	-0.86 (0.04)	12.6 (0.2)	21.1

660 [a] with simultaneous logK optimization

661 [b] with logK fixed at the weighted average value of -1.37

662 [c] mass of bacteria for EX*n* and EXA were 0.44 and 5 gL^{-1} respectively

663